Molecular Docking of Selective Hypocretin (orexin) receptor 2 Agonists: Achieving Binding Energies Exceeding –14.2 kcal/mol via Soluble and Synthetically Accessible Supramolecular Scaffolds.

Yaroslav G. Zaitsev *ORCID: 0000-0002-0069-2997 Date: 21.02.2026*

DOI: https://doi.org/10.5281/zenodo.18725152

E-mail: nabrosovnabrosov@gmail.com

Abstract

The Type II Orexin Receptor(OX2R) presents significant structural challenges that limit the development and availability of highly selective agonists. In this study, we leveraged intramolecular supramolecular interactions between core subunits to engineer a series of ligands capable of optimized volumetric filling of the receptor cavity. This was achieved through a dynamic supramolecular 'resonance sandwich' framework. These scaffolds incorporate critical orexin pharmacophores, ranging from aldehyde, carboxyl, and tetrazole groups extending deep into the pocket toward $S321^{6.52}$, as well as $T231^{5.46}$, $N324^{6.55}$, $H350^{7.39}$ and $T111^{2.61}$.

Across the entire spectrum of designed molecules, from low-molecular-weight entities to larger complexes, a unified design principle prevails: the elimination of redundant steric centers, streamlined synthesis from accessible precursors, minimal conformational hinges, and a pre-defined resonant geometry. This methodology has yielded dozens of unique compounds exhibiting exceptional affinity and selectivity. The discovery of potent water- and lipid-soluble agonists, including simple derivatives of caffeic acid, underscores the potential of this approach.

The orexin receptor (OX2R) belongs to a large family of GPCR receptors, which includes catecholamine receptors. The evolutionary ancestor of this extensive group was likely less selective and interacted with both small molecules and peptides, which likely allows for more effective use of catecholamine and aromatic profiles with increased volume. Thus, we achieved high affinity and agonistic binding without the use of direct peptide mimetics.

Keywords: Hypocretin (Orexin) Receptor 2 (OX2R), GPCR Agonism, Selective Ligand Design, O43614 (UniProt), Molecular Docking, Supramolecular Scaffolds, Intramolecular Resonance, Dynamic Resonance Sandwich, Volumetric Cavity Filling, Pre-defined Geometry, Synthetic Accessibility, Aqueous Solubility, Caffeic Acid Derivatives, Non-chiral Agonists (Steric Center Elimination), Amphiphilic Ligands.

Structural Analysis and Visual Representation of the DOX Series

To elucidate the relationship between the supramolecular architecture of the designed ligands and their binding efficiency, we present a systematic visual analysis of the DOX series (010–033). The following figures illustrate the evolution of the "resonance sandwich" concept, moving from fundamental precursors to complex, high-affinity scaffolds.
Each figure (designated as Figure DOX-XX) provides a detailed view of the ligand-receptor interface, focusing on three critical parameters:

1. **Geometric Complementarity**: The precision with which the non-chiral core subunits align with the internal topology of the OX2R pocket.
2. **Pharmacophore Vectoring**: The specific orientation of functional groups (tetrazoles, amines, or carboxyls) toward the deep-seated Serine 321 residue.
3. **Electronic Synergy**: The stabilization provided by the internal resonance within the supramolecular framework, which minimizes conformational strain during binding.

The transition from the lower-affinity molecules (e.g., DOX-01) to the lead candidate (DOX-033) demonstrates a progressive increase in volumetric cavity filling. While early structures establish the basic binding motifs, the later compounds in the series achieve a state of dynamic fit, where the ligand acts as a structural plug, maximizing van der Waals contacts and electrostatic interactions to reach affinities exceeding –14 kcal/mol.

Technical Note on Comparative Methodology

Comparative structural analysis with existing OX2R agonists was moved to the Supplementary Materials due to specific limitations in the scoring functions of standard docking algorithms. The AutoDock Vina scoring manifold often exhibits a high noise-to-signal ratio when evaluating ligands with high conformational flexibility or subtle pharmacophoric features, which frequently leads to inconsistent affinity estimations for current selective agonists.
In contrast, the DOX series was engineered with a focus on high-rigidity scaffolds and optimized volumetric filling. These structural plug characteristics provide a robust energetic signal that consistently transcends the computational noise floor of the docking tool.

Figure DOX-01

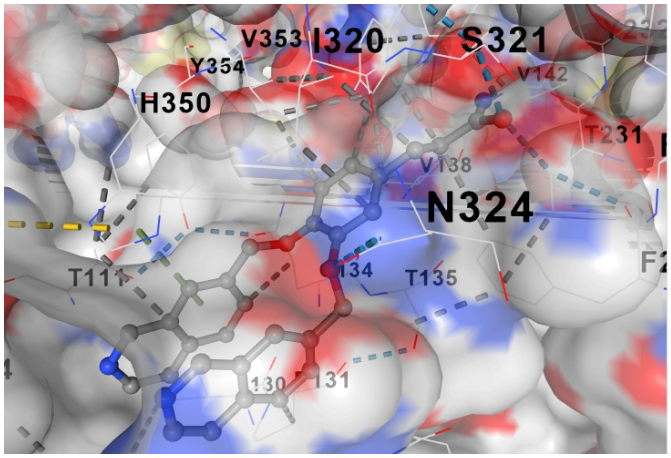

CurPocket ID	Vina score	Cavity volume (Å³)	Center (x, y, z)	Docking size (x, y, z)
C1	-11.0	1440	3, 1, -18	25, 25, 25
C2	-8.6	609	9, 14, -23	25, 25, 25
C5	-7.5	293	-21, 1, 12	25, 25, 25
			-10, -13, 4	25, 25, 25
			-38, -6, 16	25, 25, 25

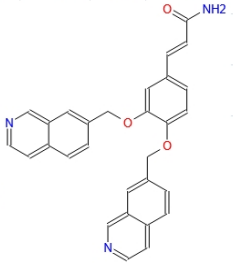

A water-soluble scaffold forming a displacing sandwich, potentially involving supramolecular and Casimir effects. This pro-catecholamine scaffold was scaled to match the dimensions of a peptidomimetic. The structure incorporates a polar agonistic amide group and terminal amine nitrogens precisely oriented within the internal receptor pocket. No agonistic interaction with the OX1R was detected, as the scaffold either occupies the upper entry vestibule or lacks contact with the receptor entrance altogether; further details are provided in the supplementary materials.

Figure DOX-02

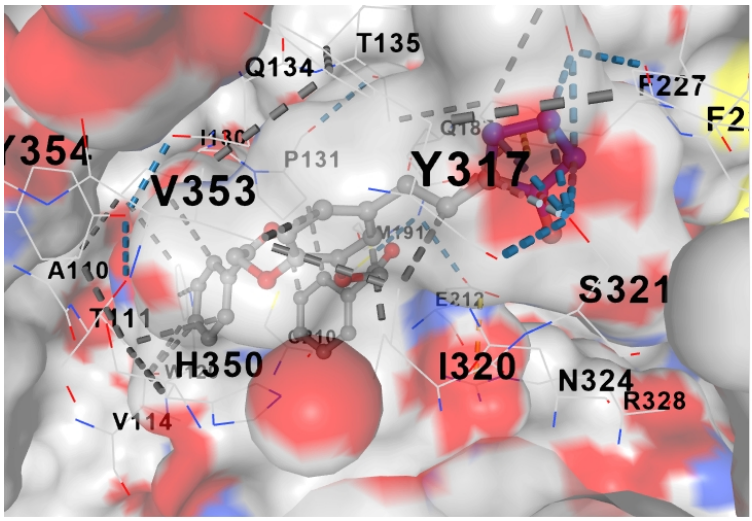

CurPocket ID	Vina score	Cavity volume (Å^3)	Center (x, y, z)	Docking size (x, y, z)
C1	-11.0	1440	3, 1, -18	24, 24, 24
C5	-7.8	293	-21, 1, 12	24, 24, 24
C2	-7.6	609	9, 14, -23	24, 24, 24
C3	-7.6	321	-10, -13, 4	24, 24, 24
C4	-7.0	296	-38, -6, 16	24, 24, 24

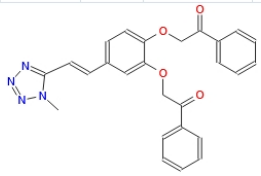

A water-soluble scaffold forming a displacing sandwich, potentially involving supramolecular and Casimir effects.
This pro-catecholamine scaffold was scaled to match the size of the peptidomimetic. The structure includes a polar agonistic tetrazole group precisely oriented within the internal receptor pocket, as well as ketone and ester pharmacophores complementary to the stabilizing amino acid residues.
No agonistic interaction with the OX1R was detected, as the scaffold either occupies the upper entry vestibule or lacks contact with the receptor entrance altogether; further details are provided in the supplementary materials.

Figure DOX-03

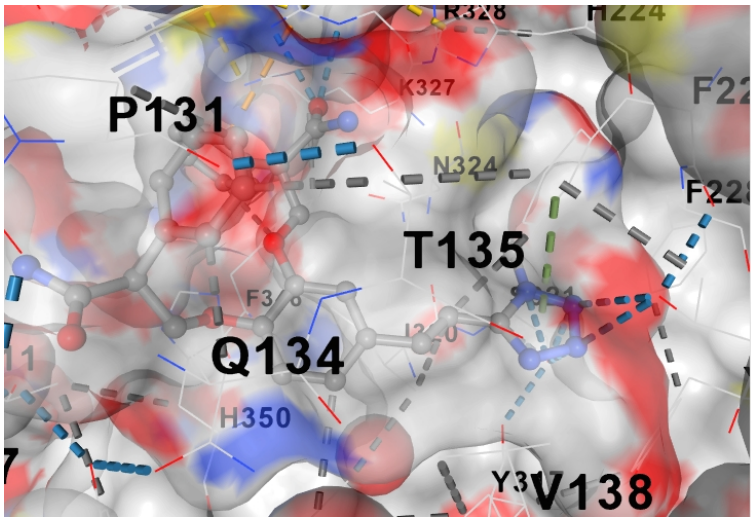

CurPocket ID	Vina score	Cavity volume (Å^3)	Center (x, y, z)	Docking size (x, y, z)
C1	-11.1	1440	3, 1, -18	26, 26, 26
C2	-7.7	609	9, 14, -23	26, 26, 26
C3	-7.6	321	-10, -13, 4	26, 26, 26
C5	-7.6	293	-21, 1, 12	26, 26, 26
C4	-6.8	296	-38, -6, 16	26, 26, 26

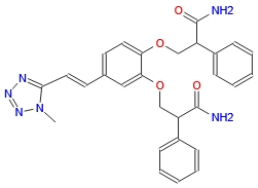

The use of tropic acid allows the structure to be supplemented with amide groups.
No agonistic interaction with the OX1R was detected, as the scaffold either occupies the upper entry vestibule or lacks contact with the receptor entrance altogether; further details are provided in the supplementary materials.

Figure DOX-04

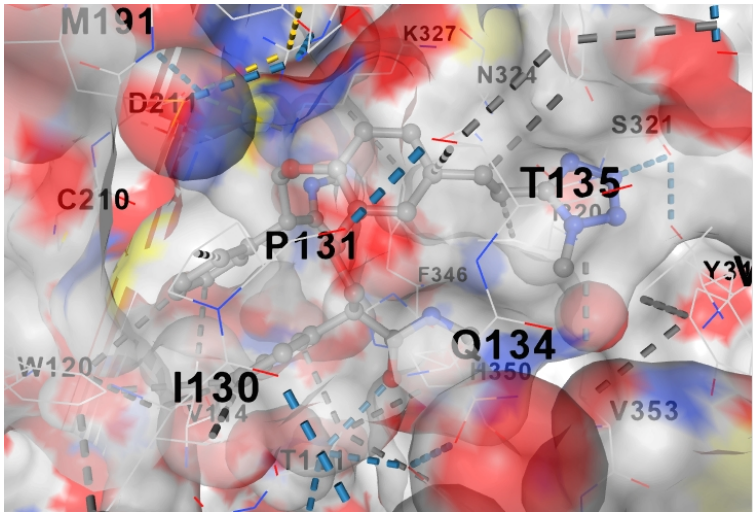

CurPocket ID	Vina score	Cavity volume (Å³)	Center (x, y, z)	Docking size (x, y, z)
C1	-11.2	1440	3, 1, -18	25, 25, 25
C5	-7.6	293	-21, 1, 12	25, 25, 25
C2	-7.2	609	9, 14, -23	25, 25, 25
C3	-6.9	321	-10, -13, 4	25, 25, 25
C4	-6.1	296	-38, -6, 16	25, 25, 25

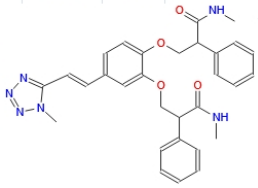

This small modification enhances the scoring value.

Figure DOX-05

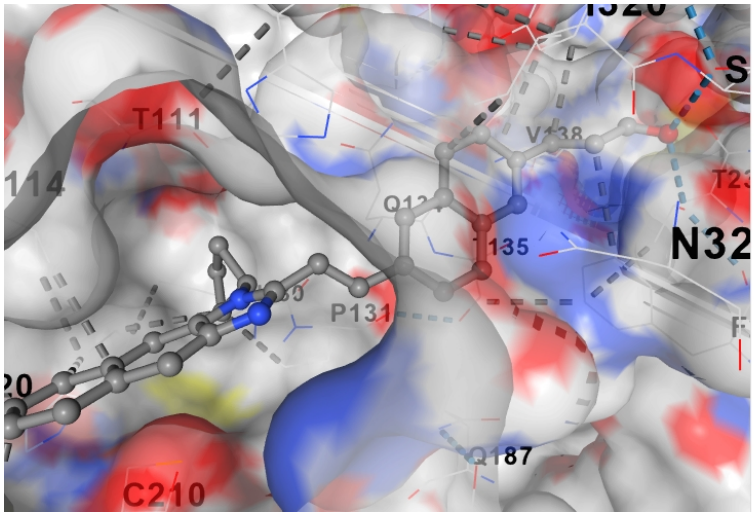

CurPocket ID	Vina score	Cavity volume (Å³)	Center (x, y, z)	Docking size (x, y, z)
C1	-11.2	1440	3, 1, -18	28, 28, 28
C2	-8.9	609	9, 14, -23	28, 28, 28
C3	-8.1	321	-10, -13, 4	28, 28, 28
C5	-7.9	293	-21, 1, 12	28, 28, 28
C4	-7.6	296	-38, -6, 16	28, 28, 28

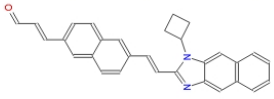

The polar aldehyde group combined with the elongated aromatic imidazole structure provides predicted water solubility and high binding affinity. As previously noted, the scaffold ensures straightforward synthetic accessibility and practical ease of handling. No agonistic interaction with the OX1R was detected, as the scaffold either occupies the upper entry vestibule or lacks contact with the receptor entrance altogether; further details are provided in the supplementary materials.

Figure DOX-06

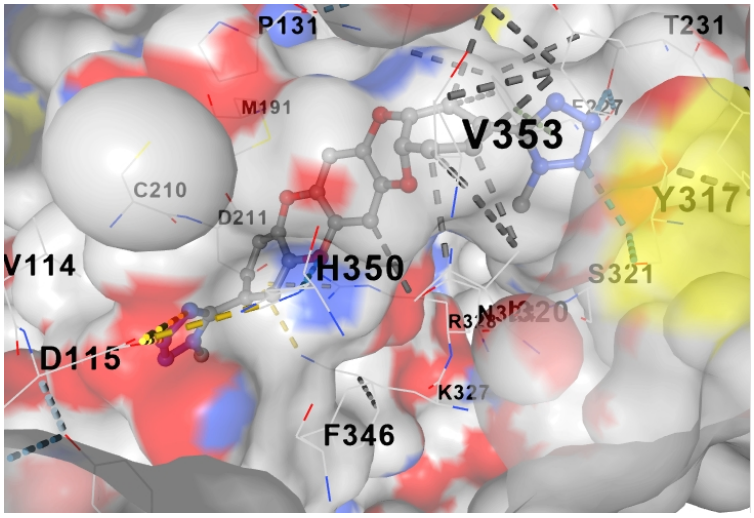

CurPocket ID	Vina score	Cavity volume (Å^3)	Center (x, y, z)	Docking size (x, y, z)
C1	-11.2	1440	3, 1, -18	26, 26, 26
C2	-10.0	609	9, 14, -23	26, 26, 26
C5	-9.8	293	-21, 1, 12	26, 26, 26
C4	-8.2	296	-38, -6, 16	26, 26, 26
C3	-7.1	321	-10, -13, 4	26, 26, 26

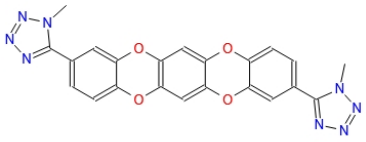

The dioxin core, featuring symmetrical tetrazole moieties, extends the logic of the extended monolayer vector; it incorporates both a deep-pocket-binding agonistic tetrazole and a tail-anchoring tetrazole group. No agonistic interaction with the OX1R was detected, as the scaffold either occupies the upper entry vestibule or lacks contact with the receptor entrance altogether; further details are provided in the supplementary materials.

Figure DOX-07

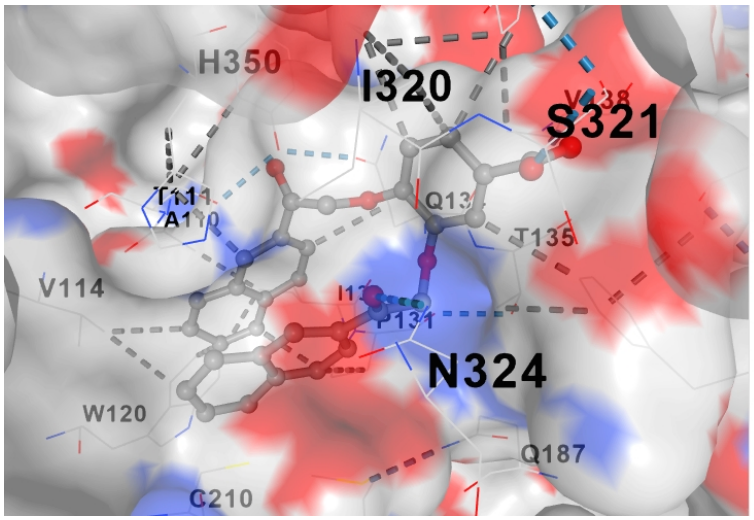

CurPocket ID	Vina score	Cavity volume (Å^3)	Center (x, y, z)	Docking size (x, y, z)
C1	-11.2	1440	3, 1, -18	23, 23, 23
C2	-9.0	609	9, 14, -23	23, 23, 23
C5	-8.1	293	-21, 1, 12	23, 23, 23
C3	-7.1	321	-10, -13, 4	23, 23, 23
			-6, 16	23, 23, 23

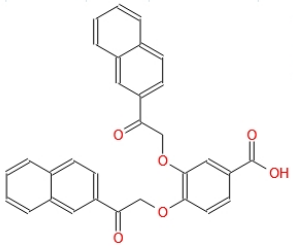

A bilayered naphthyl-based lipophilic scaffold, featuring a carboxyl agonist group targeting the deep pocket, exhibits comparable affinity. The carboxyl group can be delivered across the blood-brain barrier (BBB) as an ester; such esters often demonstrate enhanced affinity and a pronounced initial potency, a characteristic feature of these scaffolds. No agonistic interaction with the OX1R was detected, as the scaffold either occupies the upper entry vestibule or lacks contact with the receptor entrance altogether; further details are provided in the supplementary materials.

Figure DOX-08

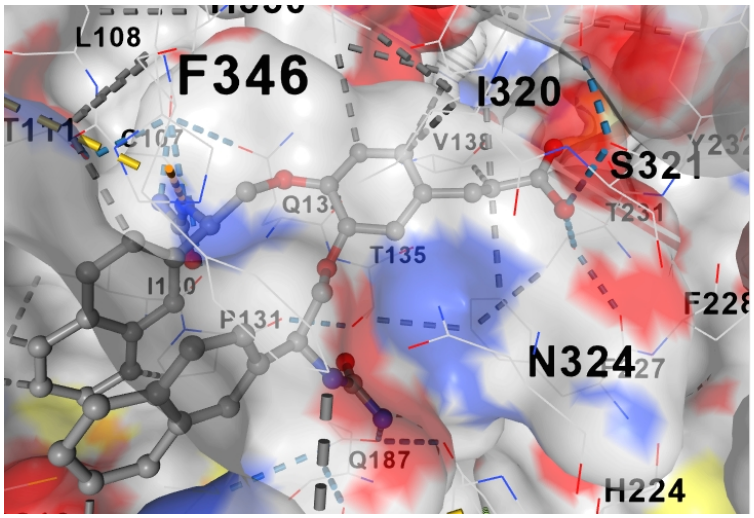

CurPocket ID	Vina score	Cavity volume (Å³)	Center (x, y, z)	Docking size (x, y, z)
C1	-11.8	1440	3, 1, -18	27, 27, 27
C2	-9.5	609	9, 14, -23	27, 27, 27
C5	-8.5	293	-21, 1, 12	27, 27, 27
C3	-7.1	321	-10, -13, 4	27, 27, 27
			-38, -6, 16	27, 27, 27

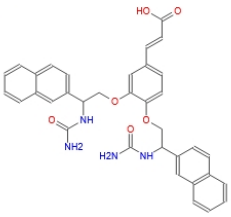

A bilayered scaffold, enriched with naphthyl and urea groups in the central region of the molecule, exhibits enhanced affinity. The transition to a caffeic acid moiety established a rigid vector, facilitating deep penetration into the receptor's agonist binding pocket. To ensure permeability, the carboxyl group can be delivered across the blood-brain barrier (BBB) as an ester; such esters often demonstrate higher affinity and a rapid onset of action, a hallmark of this scaffold series.
No agonistic interaction with the OX1R was detected, as the scaffold either occupies the upper entry vestibule or lacks contact with the receptor entrance altogether; further details are provided in the supplementary materials.

Figure DOX-09

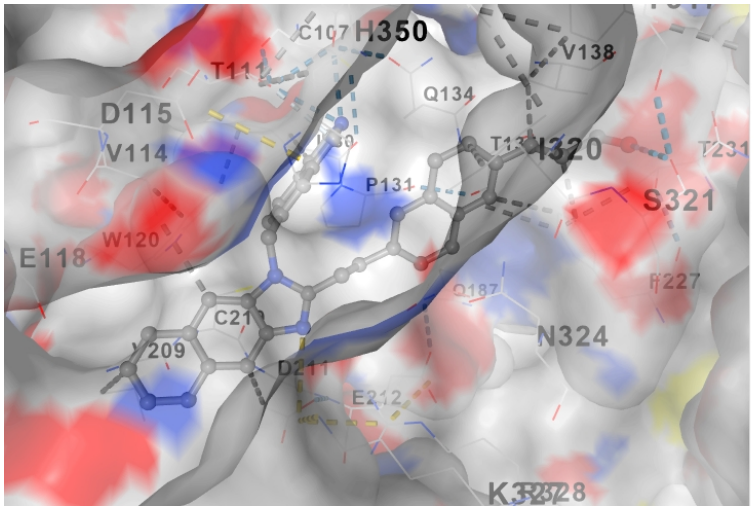

CurPocket ID	Vina score	Cavity volume (Å³)	Center (x, y, z)	Docking size (x, y, z)
C1	-11.8	1440	3, 1, -18	27, 27, 27
C2	-9.8	609	9, 14, -23	27, 27, 27
C5	-9.4	293	-21, 1, 12	27, 27, 27
		321	-10, -13, 4	27, 27, 27
		296	-38, -6, 16	27, 27, 27

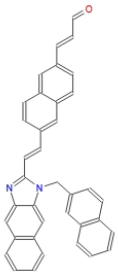

The polar aldehyde group, in combination with the elongated imidazole-based aromatic structure, provides limited water solubility alongside high binding affinity. Furthermore, the framework offers straightforward synthetic accessibility and ease of handling. No agonistic interaction with the OX1R

was detected, as the scaffold either occupies the upper entry vestibule or lacks contact with the receptor entrance altogether; further details are provided in the supplementary materials.

Figure DOX-010

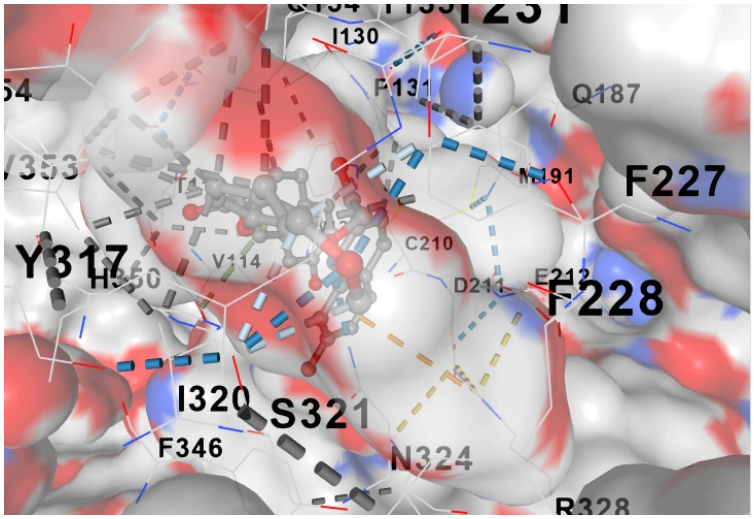

CurPocket ID	Vina score	Cavity volume (Å³)	Center (x, y, z)	Docking size (x, y, z)
C1	-11.9	1440	3, 1, -18	26, 26, 26
C2	-9.0	609	9, 14, -23	26, 26, 26
C3	-8.1	321	-10, -13, 4	26, 26, 26
			-21, 1, 12	26, 26, 26
			-38, -6, 16	26, 26, 26

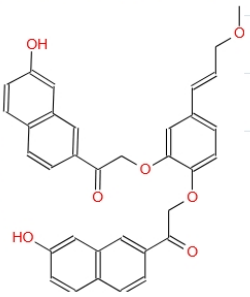

The transition to a bilayered architecture, featuring a cinnamyl alcohol ester as an agonistic 'anchor' pharmacophore and structure-stabilizing naphthol hydroxyl groups, enhances the binding affinity of the lipophilic core. Within the receptor pocket, the hydroxyls of the aromatic moiety in an inverted orientation are capable of binding the Serine 315 residue. While sandwich structures in this reverse arrangement typically exhibit lower affinity and less stable configurations, the risk of diminished selectivity remains.

Figure DOX-011

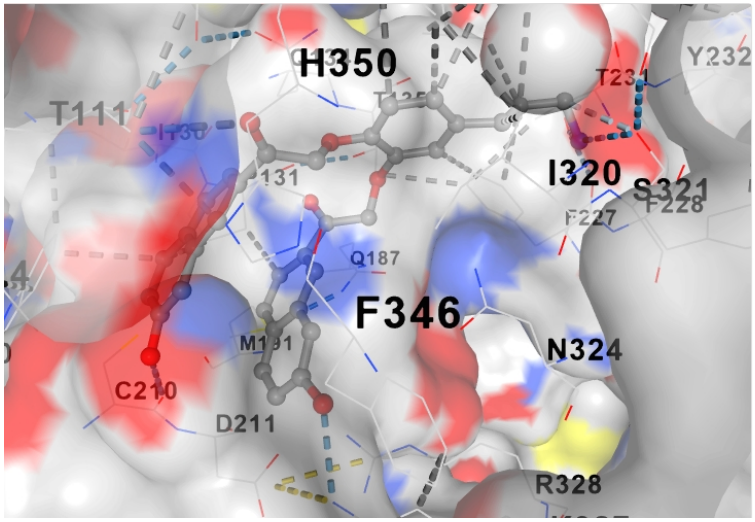

CurPocket ID	Vina score	Cavity volume (Å³)	Center (x, y, z)	Docking size (x, y, z)
C1	-12.1	1440	3, 1, -18	24, 24, 24
C2	-8.8	609	9, 14, -23	24, 24, 24
C5	-8.7	293	-21, 1, 12	24, 24, 24
			4	24, 24, 24
			16	24, 24, 24

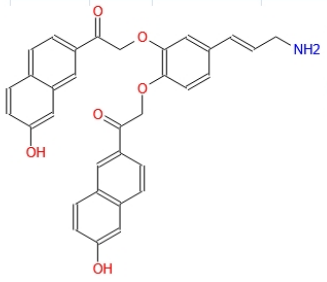

Switching from an ether to a primary amine increased the affinity. When positioned within the pocket in an inverted orientation, hydroxyls in the aromatic moiety are capable of binding to the Serine 315 residue. Although sandwich structures in this reverse arrangement often exhibit lower affinity and less stable configurations, the risk of low selectivity remains.

Figure DOX-012

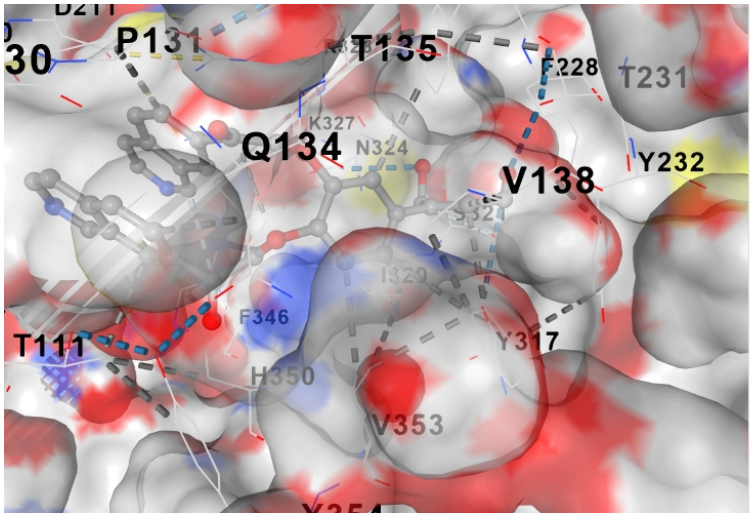

CurPocket ID	Vina score	Cavity volume (Å³)	Center (x, y, z)	Docking size (x, y, z)
C1	-12.1	1440	3, 1, -18	26, 26, 26
C3	-9.1	321	-10, -13, 4	26, 26, 26
C2	-8.8	609	9, 14, -23	26, 26, 26
			-21, 1, 12	26, 26, 26
			-38, -6, 16	26, 26, 26

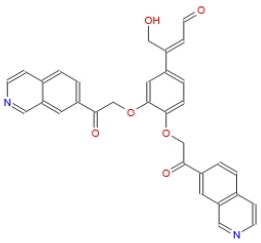

The implementation of a dual interaction within the agonist binding site, combined with the enhanced water solubility of the sandwich structure, maintains binding affinity at a comparable level.
No agonistic interaction with the OX1R was detected, as the scaffold either occupies the upper entry vestibule or lacks contact with the receptor entrance altogether; further details are provided in the supplementary materials.

Figure DOX-013

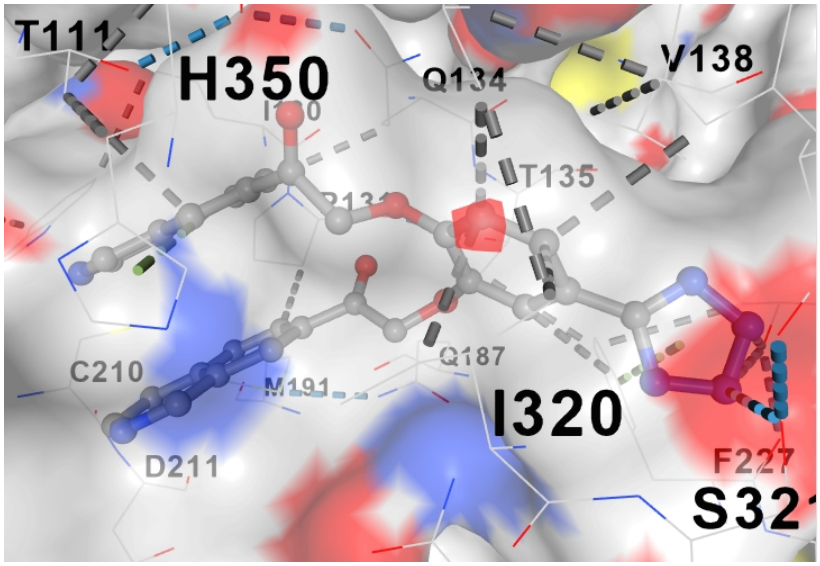

CurPocket ID	Vina score	Cavity volume (Å³)	Center (x, y, z)
C1	-12.1	1440	3, 1, -18
C2	-10.3	609	9, 14, -23
C3	-8.2	321	-10, -13, 4
C4	-8.0	296	-38, -6, 16
			21, 1, 12

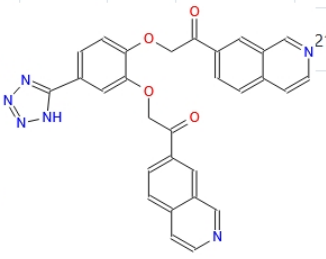

The tetrazole-based scaffold exhibits enhanced water solubility while maintaining a comparable level of affinity. The involvement of the tetrazole ring in anion–π interactions may be a key determinant of binding stability and potential agonistic efficacy. Furthermore, the methylated tetrazole pharmacophore generally provides a more pronounced increase in binding affinity.

Figure DOX-014

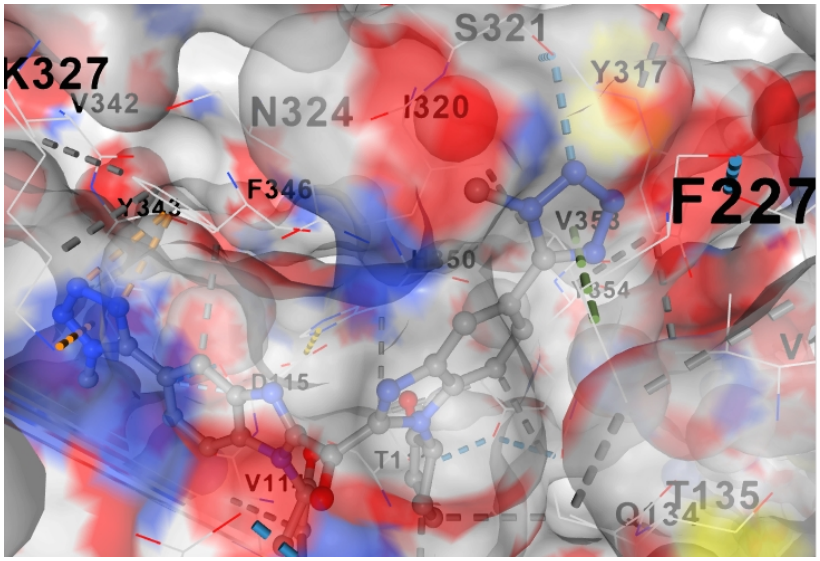

CurPocket ID	Vina score	Cavity volume (Å³)	Center (x, y, z)
C1	-12.1	1440	3, 1, -18
C5	-9.8	293	-21, 1, 12
C2	-8.9	609	9, 14, -23
C4	-8.1	296	-38, -6, 16
			-13, 4

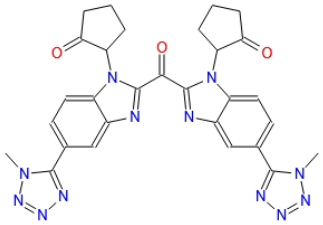

A benzimidazole-tetrazole dimer with controlled asymmetry demonstrates a straightforward implementation of a peptidomimetic directed into the receptor cavity. The tetrazole acts as both an apical agonist pharmacophore and a tail anchor, while the cyclopentanone moieties complement the mimetic activity in the central portion of the structure. High water solubility does not compromise the previously achieved affinity. No agonistic interaction with the OX1R was detected, as the scaffold either occupies the upper entry vestibule or lacks contact with the receptor entrance altogether; further details are provided in the supplementary materials.

Figure DOX-015

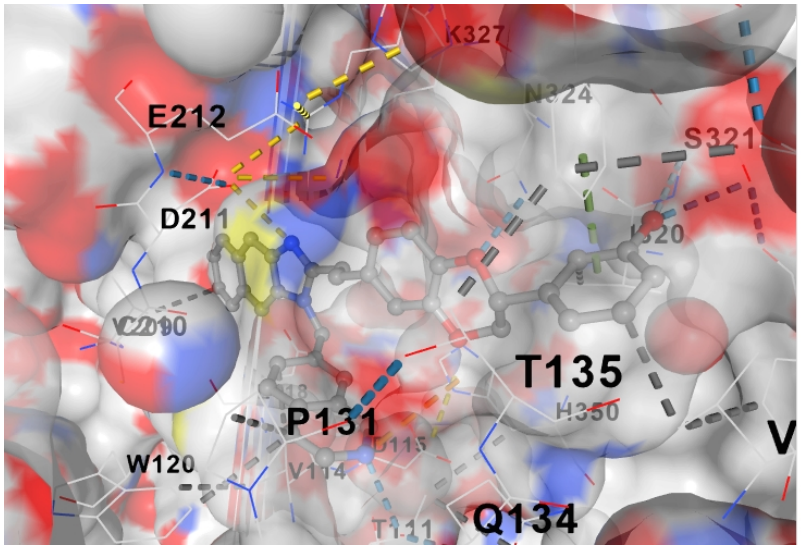

CurPocket ID	Vina score	Cavity volume (Å³)	Center (x, y, z)
C1	-12.2	1440	3, 1, -18
C2	-11.5	609	9, 14, -23
C5	-9.8	293	-21, 1, 12
	-8.6	296	-38, -6, 16
	-8.3	321	-10, -13, 4

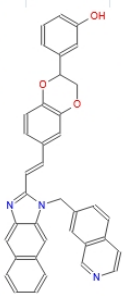

The benzodioxane bridge, supporting the agonistic meta-hydroxybenzene group, serves as a unique rotating element that defines the binding mode deep within the pockets of both orexin receptor types. However, only the optimal positioning within the type 2 receptor cavity enables these structures to act as selective OX2R agonists. Establishing true selectivity requires further validation using refined docking models and in vitro assays.

Figure DOX-016

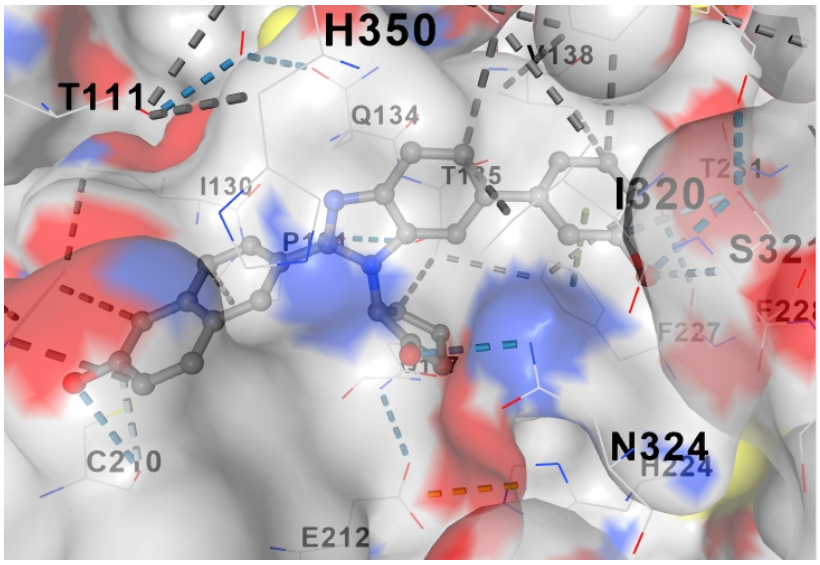

CurPocket ID	Vina score	Cavity volume (Å^3)	Center (x, y, z)
C1	-12.2	1440	3, 1, -18
C2	-9.6	609	9, 14, -23
C5	-9.6	293	-21, 1, 12
C3	-7.6	321	-10, -13, 4
C4	-7.4	296	-38, -6, 16

The compact benzimidazole derivative bearing two phenolic groups exhibits comparable affinity to the previous structure; however, its selectivity profile warrants further rigorous validation.

Figure DOX-017

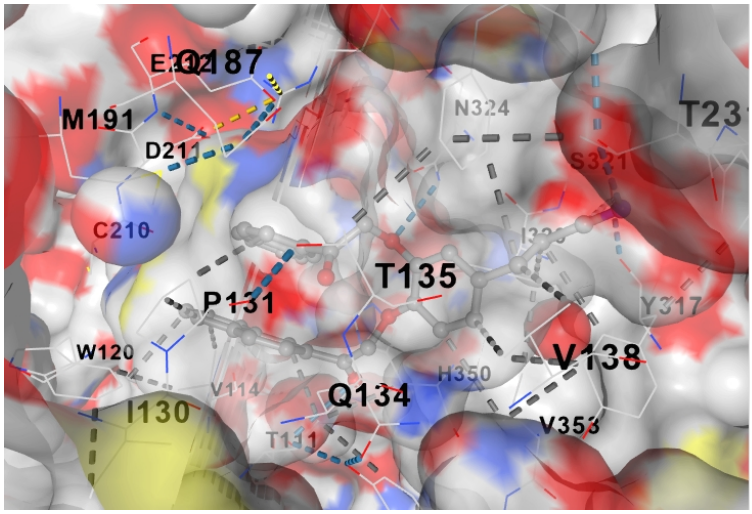

CurPocket ID	Vina score	Cavity volume (Å^3)	Center (x, y, z)	Docking size (x, y, z)
C1	-12.2	1440	3, 1, -18	25, 25, 25
C2	-8.8	609	9, 14, -23	25, 25, 25
C5	-7.1	293	-21, 1, 12	25, 25, 25
		321	-10, -13, 4	25, 25, 25
		296	-38, -6, 16	25, 25, 25

The lipid-soluble sandwich structure exhibits affinity comparable to previous scaffolds; the nitrile agonist group serves as a distinctive feature of this lipophilic and neutral scaffold.

No agonistic interaction with the OX1R was detected, as the scaffold either occupies the upper entry vestibule or lacks contact with the receptor entrance altogether; further details are provided in the supplementary materials.

Figure DOX-018

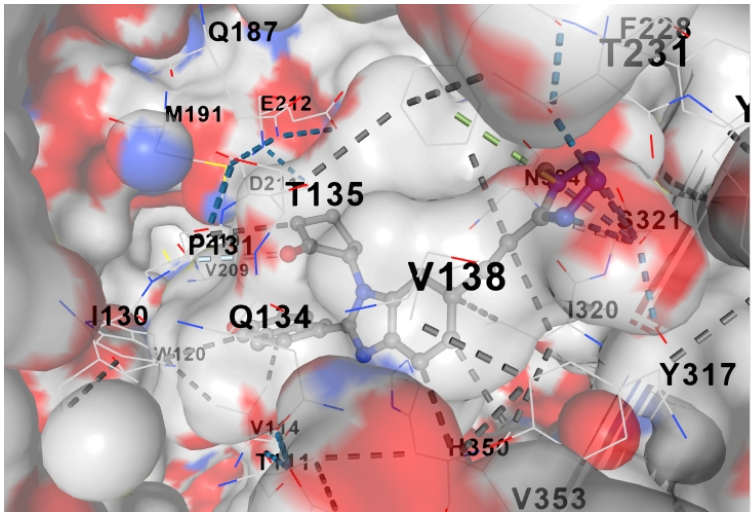

CurPocket ID	Vina score	Cavity volume (Å^3)	Center (x, y, z)	Docking size (x, y, z)
C1	-12.3	1440	3, 1, -18	26, 26, 26
C2	-9.2	609	9, 14, -23	26, 26, 26
C5	-9.1	293	-21, 1, 12	26, 26, 26
C4	-7.4	296	-38, -6, 16	26, 26, 26
C3	-7.3	321	-10, -13, 4	26, 26, 26

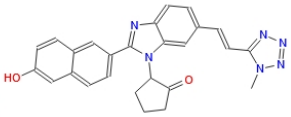

A compact benzimidazole derivative bearing a phenolic group exhibits higher affinity than the preceding compound; however, its selectivity profile warrants further rigorous verification.

Figure DOX-019

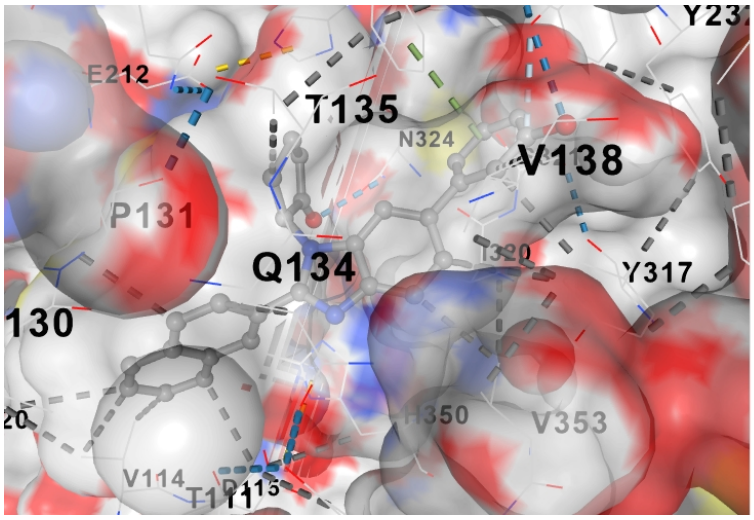

CurPocket ID	Vina score	Cavity volume (Å^3)	Center (x, y, z)	Docking size (x, y, z)
C1	-12.3	1440	3, 1, -18	24, 24, 24
C2	-9.4	609	9, 14, -23	24, 24, 24
C5	-9.3	293	-21, 1, 12	24, 24, 24
C3	-8.1	321	-10, -13, 4	24, 24, 24
C4	-7.5	296	-38, -6, 16	24, 24, 24

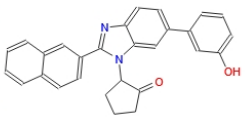

A compact benzimidazole derivative containing a phenolic group exhibits comparable affinity; however, its selectivity profile also warrants further rigorous validation.

Figure DOX-020

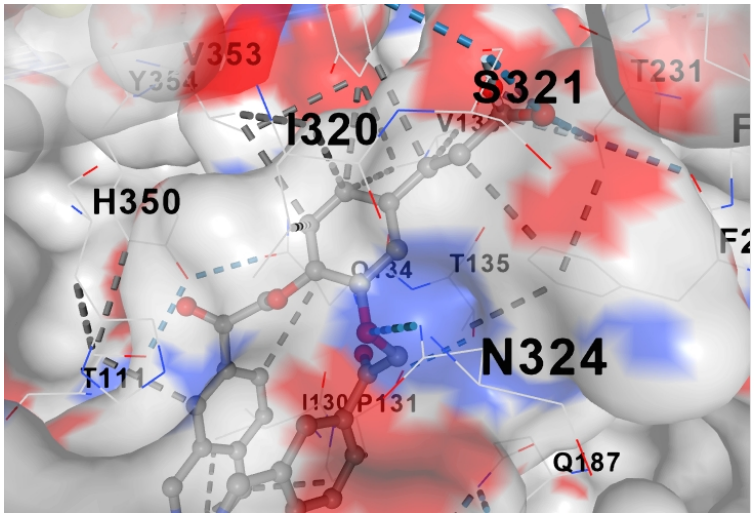

CurPocket ID	Vina score	Cavity volume (Å³)	Center (x, y, z)	Docking size (x, y, z)
C1	-12.3	1440	3, 1, -18	26, 26, 26
C5	-8.8	293	-21, 1, 12	26, 26, 26
C4	-7.1	296	-38, -6, 16	26, 26, 26
				26, 26, 26
				26, 26, 26

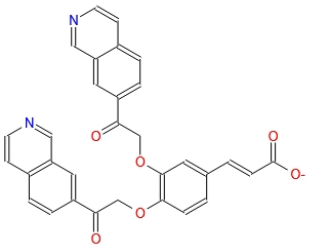

A bilayered scaffold, based on isoquinoline groups, exhibits enhanced affinity. The transition to a caffeic acid moiety established a rigid vector, facilitating deep penetration into the receptor's agonist binding pocket. To ensure permeability, the carboxyl group can be delivered across the blood-brain barrier (BBB) as an ester; such esters often demonstrate higher affinity and a rapid onset of action, a hallmark of this scaffold series.
No agonistic interaction with the OX1R was detected, as the scaffold either occupies the upper entry vestibule or lacks contact with the receptor entrance altogether; further details are provided in the supplementary materials.

Figure DOX-021

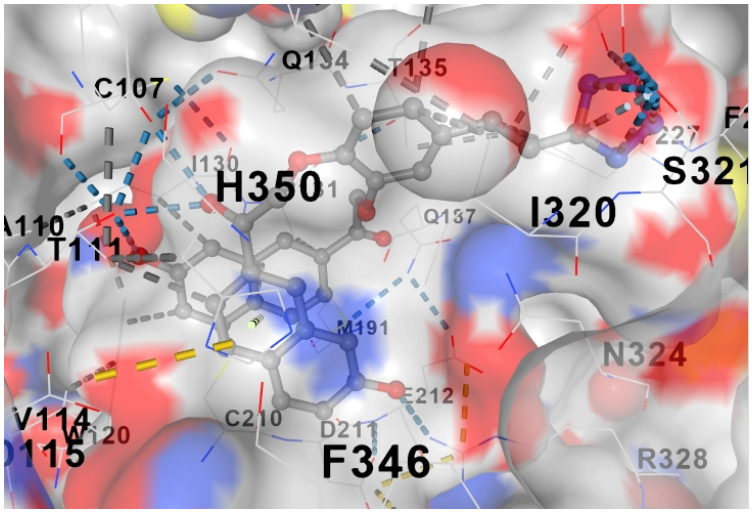

CurPocket ID	Vina score	Cavity volume (Å³)	Center (x, y, z)	Docking size (x, y, z)
C1	-12.4	1440	3, 1, -18	29, 29, 29
C2	-10.0	609	9, 14, -23	29, 29, 29
C3	-9.0	321	-10, -13, 4	29, 29, 29
				29, 29, 29
				29, 29, 29

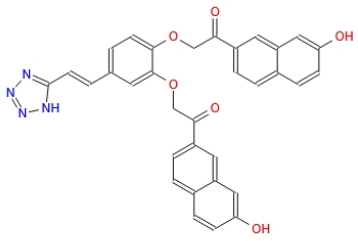

The incorporation of a tetrazole moiety increases binding affinity, but the hydroxyl groups of the naphthyl sandwich require more rigorous selectivity testing.

Figure DOX-022

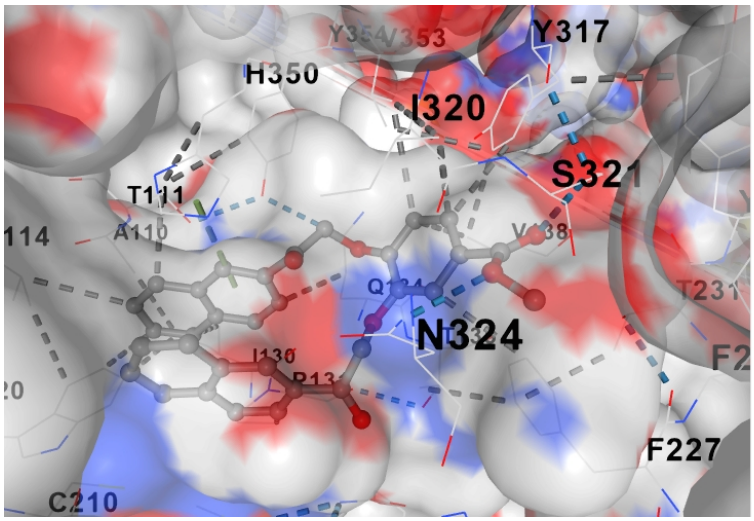

CurPocket ID	Vina score	Cavity volume (Å³)	Center (x, y, z)	Docking size (x, y, z)
C1	-12.4	1440	3, 1, -18	25, 25, 25
C5	-8.4	293	-21, 1, 12	25, 25, 25
C3	-7.6	321	-10, -13, 4	25, 25, 25
				25, 25, 25
				25, 25, 25

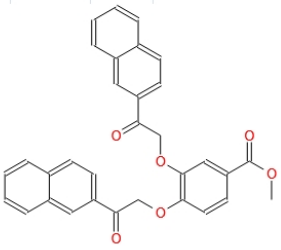

A lipophilic, hydroxyl-free scaffold featuring an agonistic ester group maintains affinity comparable to that of the previous structure. No agonistic interaction with the OX1R was detected, as the scaffold either occupies the upper entry vestibule or lacks contact with the receptor entrance altogether; further details are provided in the supplementary materials.

Figure DOX-023

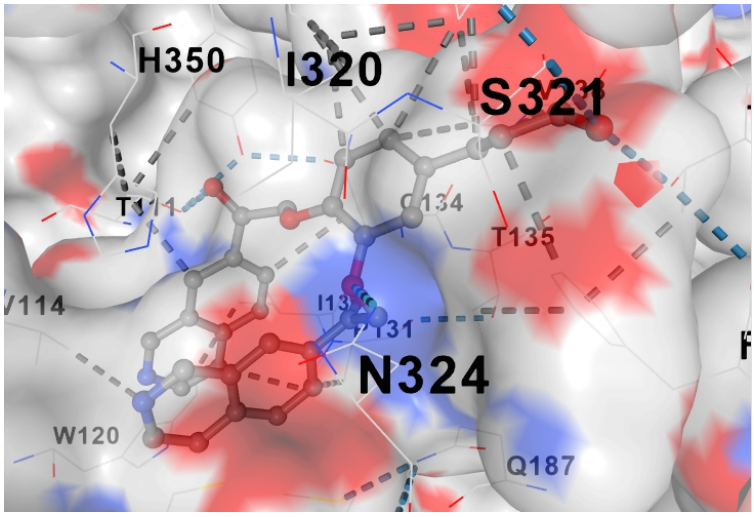

CurPocket ID	Vina score	Cavity volume (Å³)	Center (x, y, z)	Docking size (x, y, z)
C1	-12.4	1440	3, 1, -18	26, 26, 26
C2	-8.0	609	9, 14, -23	26, 26, 26
C3	-7.5	321	-10, -13, 4	26, 26, 26
				26, 26, 26
				26, 26, 26

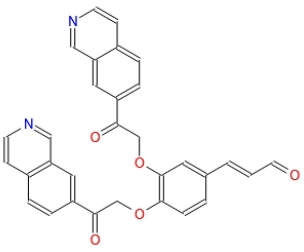

A bilayered scaffold, based on isoquinoline groups, exhibits enhanced affinity. The transition to a caffeic aldehyde moiety established a rigid vector, facilitating deep penetration into the receptor's agonist binding pocket. No agonistic interaction with the OX1R was detected, as the scaffold either occupies the upper entry vestibule or lacks contact with the receptor entrance altogether; further details are provided in the supplementary materials.

Figure DOX-024

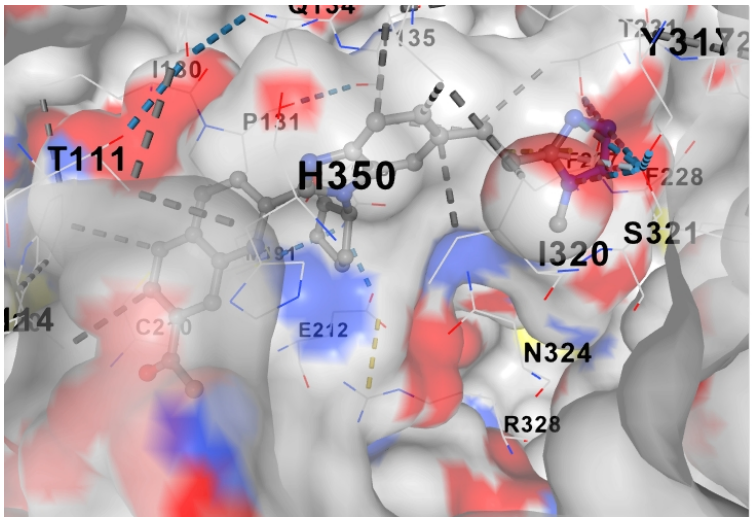

CurPocket ID	Vina score	Cavity volume (Å^3)	Center (x, y, z)	Docking size (x, y, z)
C1	-12.5	1440	3, 1, -18	26, 26, 26
C2	-10.0	609	9, 14, -23	26, 26, 26
C5	-9.2	293	-21, 1, 12	26, 26, 26
C3	-8.0	321	-10, -13, 4	26, 26, 26
C4	-7.5	296	-38, -6, 16	26, 26, 26

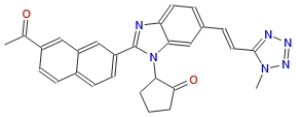

A compact benzimidazole-tetrazole derivative containing phenolic group exhibits superior affinity to the previous structure. No agonistic interaction with the OX1R was detected, as the scaffold either occupies the upper entry vestibule or lacks contact with the receptor entrance altogether; further details are provided in the supplementary materials.

Figure DOX-025

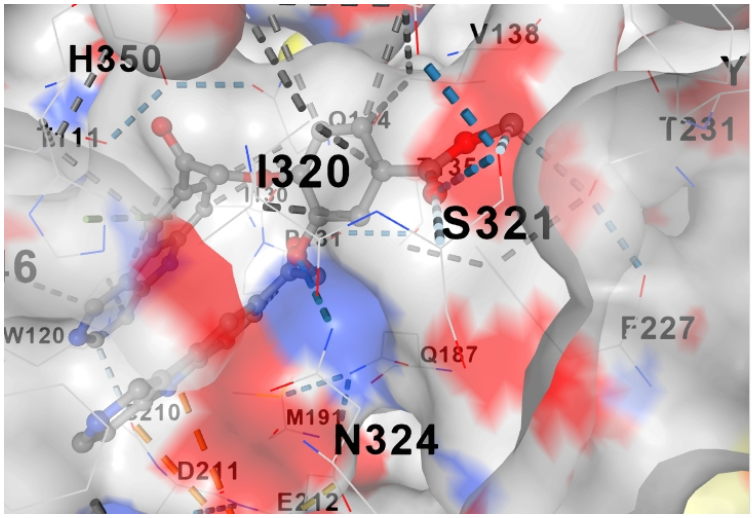

CurPocket ID	Vina score	Cavity volume (Å^3)	Center (x, y, z)	Docking size (x, y, z)
C1	-12.5	1440	3, 1, -18	28, 28, 28
C2	-10.2	609	9, 14, -23	28, 28, 28
C5	-9.4	293	-21, 1, 12	28, 28, 28
				28, 28, 28
				28, 28, 28

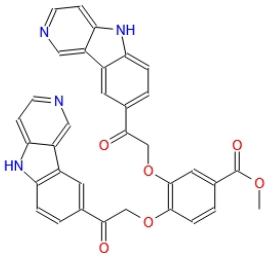

A sandwich scaffold based on a carbazole-amine derivative and 3,4-dihydroxybenzoic acid methyl ester exhibits affinity comparable to the previous structure, while maintaining high water solubility. No agonistic interaction with the OX1R was detected, as the scaffold either occupies the upper entry vestibule or lacks contact with the receptor entrance altogether; further details are provided in the supplementary materials.

Figure DOX-026

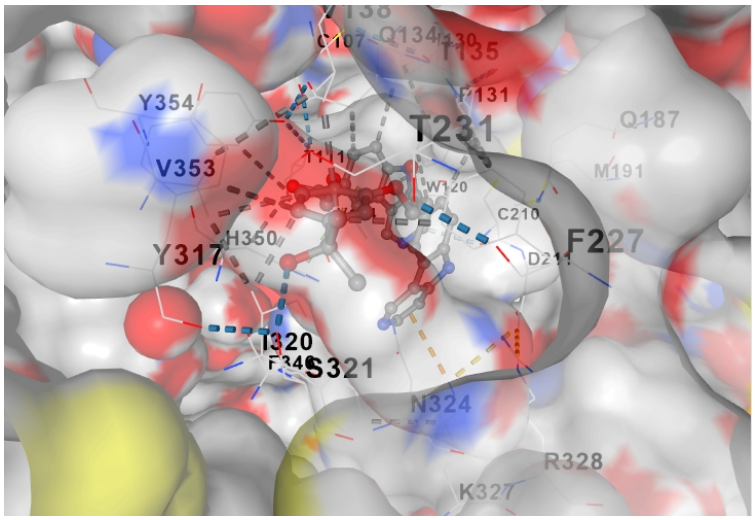

CurPocket ID	Vina score	Cavity volume (Å³)	Center (x, y, z)	Docking size (x, y, z)
C1	-12.6	1440	3, 1, -18	24, 24, 24
C2	-9.6	609	9, 14, -23	24, 24, 24
C3	-8.7	321	-10, -13, 4	24, 24, 24
			-21, 1, 12	24, 24, 24
			-38, -6, 16	24, 24, 24

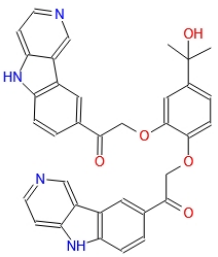

A derivative featuring a tertiary alcoholic agonist moiety exhibits enhanced binding affinity.
No agonistic interaction with the OX1R was detected, as the scaffold either occupies the upper entry vestibule or lacks contact with the receptor entrance altogether; further details are provided in the supplementary materials.

Figure DOX-027

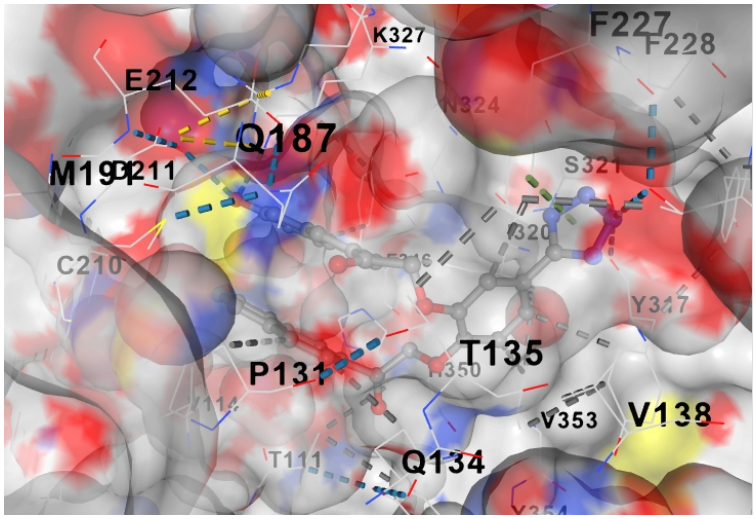

CurPocket ID	Vina score	Cavity volume (Å³)	Center (x, y, z)	Docking size (x, y, z)
C1	-12.7	1440	3, 1, -18	28, 28, 28
C5	-8.8	293	-21, 1, 12	28, 28, 28
C3	-8.4	321	-10, -13, 4	28, 28, 28
C2	-7.8	609	9, 14, -23	28, 28, 28
			-38, -6, 16	28, 28, 28

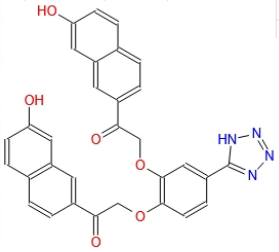

Switching to an unsubstituted agonistic tetrazole and a lipophilic hydroxylated naphthalene moiety increases the binding affinity; however, its selectivity profile warrants further rigorous validation.

Figure DOX-028

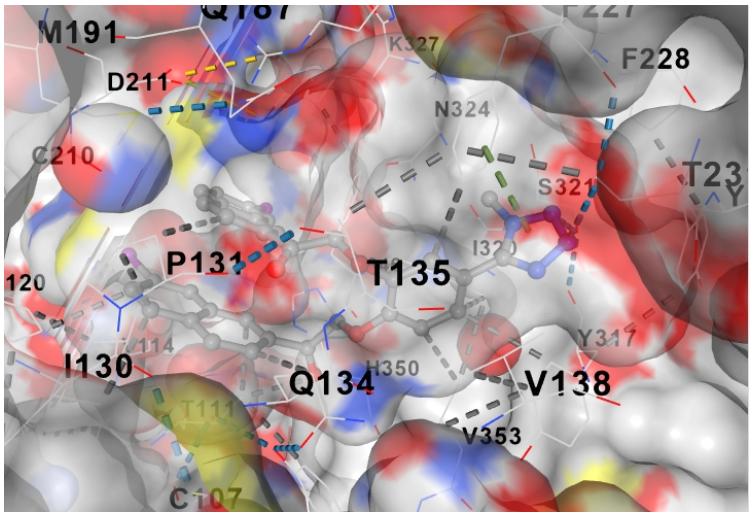

CurPocket ID	Vina score	Cavity volume (Å^3)	Center (x, y, z)	Docking size (x, y, z)
C1	-13.1	1440	3, 1, -18	26, 26, 26
C2	-9.3	609	9, 14, -23	26, 26, 26
C3	-8.7	321	-10, -13, 4	26, 26, 26
C4	-7.8	296	-38, -6, 16	26, 26, 26
			-21, 1, 12	26, 26, 26

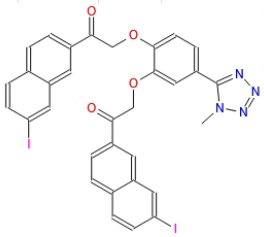

The iodinated derivative sets a new benchmark for affinity among known analogs and exhibits no detectable binding within the OX1R pocket. No agonistic interaction with the OX1R was detected, as the scaffold either occupies the upper entry vestibule or lacks contact with the receptor entrance altogether; further details are provided in the supplementary materials.

Figure DOX-029

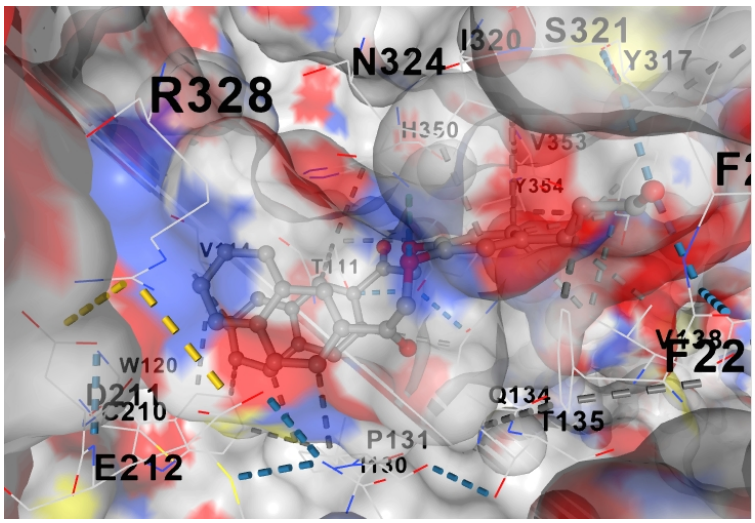

CurPocket ID	Vina score	Cavity volume (Å^3)	Center (x, y, z)	Docking size (x, y, z)
C1	-13.2	1440	3, 1, -18	26, 26, 26
C2	-9.7	609	9, 14, -23	26, 26, 26
C3	-8.7	321	-10, -13, 4	26, 26, 26
		293	-21, 1, 12	26, 26, 26
		296	-38, -6, 16	26, 26, 26

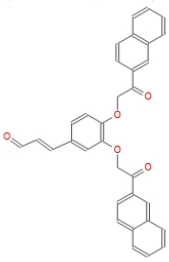

A lipophilic derivative of caffeic aldehyde exhibits high affinity alongside straightforward synthetic accessibility. No agonistic interaction with the OX1R was detected, as the scaffold either occupies the upper entry vestibule or lacks contact with the receptor entrance altogether; further details are provided in the supplementary materials.

Figure DOX-030

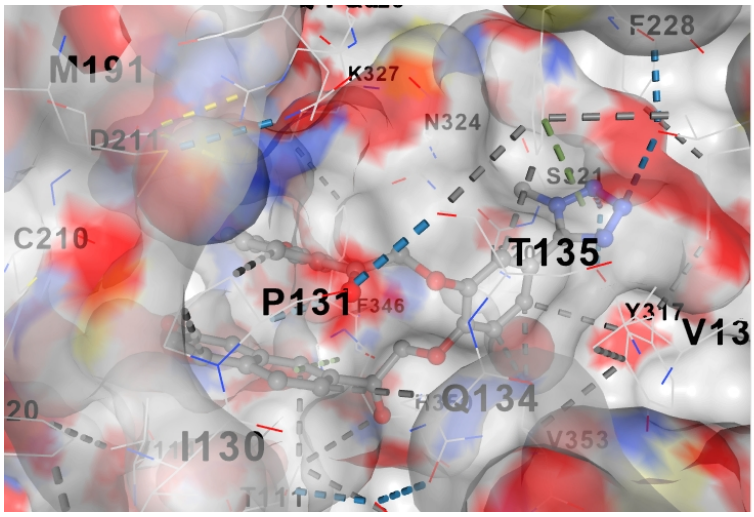

CurPocket ID	Vina score	Cavity volume (Å^3)	Center (x, y, z)	Docking size (x, y, z)
C1	-13.2	1440	3, 1, -18	26, 26, 26
C2	-8.4	609	9, 14, -23	26, 26, 26
C5	-7.6	293	-21, 1, 12	26, 26, 26
				26, 26, 26
				26, 26, 26

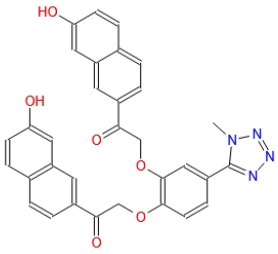

Substitution with a hydroxylated aromatic core and methyl tetrazole maintains high affinity while providing the structure with a favorable water-soluble amphiphilic profile; however, its selectivity profile warrants further rigorous validation.

Figure DOX-031

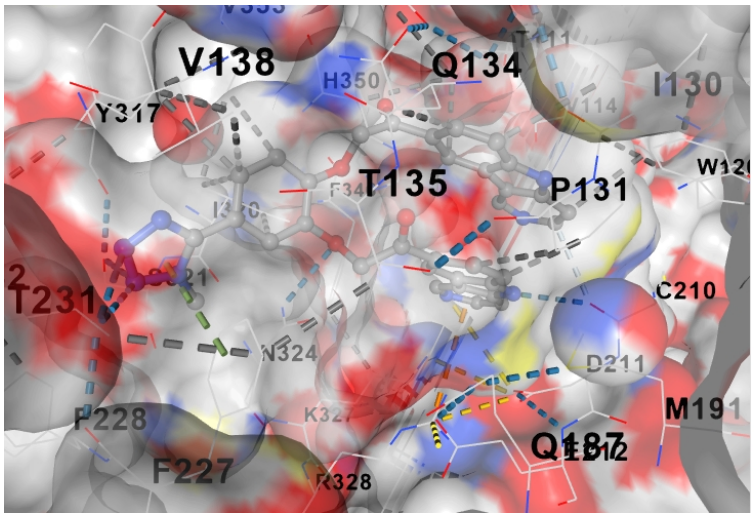

CurPocket ID	Vina score	Cavity volume (Å^3)	Center (x, y, z)	Docking size (x, y, z)
C1	-13.2	1440	3, 1, -18	27, 27, 27
C2	-9.5	609	9, 14, -23	27, 27, 27
C5	-9.1	293	-21, 1, 12	27, 27, 27
				27, 27, 27
				27, 27, 27

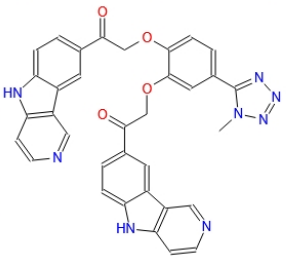

A sandwich scaffold based on a carbazole-amine derivative exhibits affinity comparable to the previous structure, while maintaining high water solubility. No agonistic interaction with the OX1R was detected, as the scaffold either occupies the upper entry vestibule or lacks contact with the receptor entrance altogether; further details are provided in the supplementary materials.

Figure DOX-032

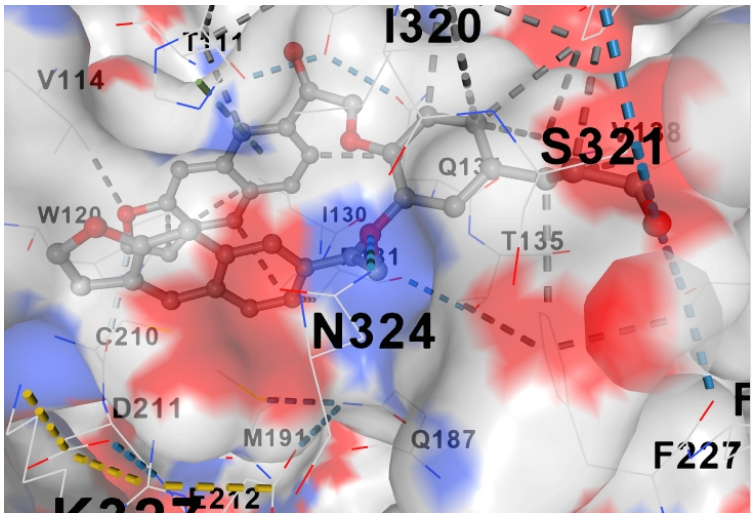

CurPocket ID	Vina score	Cavity volume (Å³)	Center (x, y, z)	Docking size (x, y, z)
C1	-13.8	1440	3, 1, -18	27, 27, 27
C2	-10.2	609	9, 14, -23	27, 27, 27
C5	-8.2	293	-21, 1, 12	27, 27, 27
				27, 27, 27
				27, 27, 27

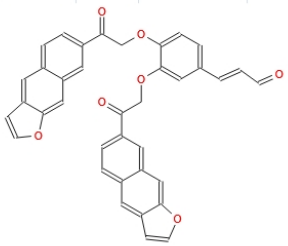

A lipophilic sandwich structure, based on a naphthylfuran tricycle and caffeic aldehyde, demonstrates an unprecedented level of affinity, establishing a new benchmark for toxicological and efficacy assessment. Molecular docking simulations reveal extensive pocket occupancy and high structural conformity, as well as a phase shift within the sandwich architecture, transforming the geometry into a mobile wedge-like configuration.

Figure DOX-033

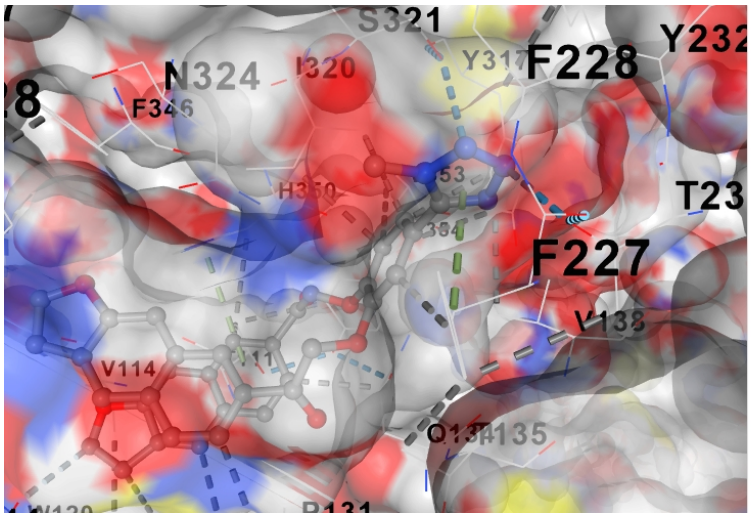

CurPocket ID	Vina score	Cavity volume (Å³)	Center (x, y, z)	Docking size (x, y, z)
C1	-14.2	1440	3, 1, -18	27, 27, 27
C2	-10.4	609	9, 14, -23	27, 27, 27
C5	-9.3	293	-21, 1, 12	27, 27, 27
				27, 27, 27
				27, 27, 27

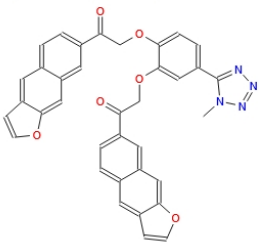

The methyl tetrazole derivative increases affinity to the limits of practical pharmacology. This confirms a consistent correlation between binding strength and the increasing effective molecular mass of these sandwich scaffolds.

Concluding Remarks:

This work demonstrates the consistently superior efficiency of the developed supramolecular 'sandwich' pharmacological strategy. Leveraging dynamic complementarity and the unique properties of cyclic spatial scaffolds enables the design of volumetric, click-chemistry-derived pseudo-peptidomimetics.

The specific physics of the parallel slabs within these cyclic sandwiches may not be fully captured by standard molecular docking, as supramolecular and Casimir-like effects can predominate at sub-nanometer scales. This positions the proposed strategy in the realm of macroquantum interactions, necessitating further refinement using high-precision docking tools and comprehensive biological assays.

The supplementary materials include visualizations of dozens of additional structures with affinities ranging from –8to –14.2 kcal/mol. These materials provide comprehensive docking data, interactive HTML reports, and videos demonstrating volumetric renderings of the complexes.

Methods

Since the study requires a model of the receptor in its native conformational state, the AlphaFold Monomer v2.0 predictions for the Human Orexin Receptor Type 2 (O43614) and Orexin Receptor Type 1 (A6NMV7) were utilized as the receptor models. These models provide a high-confidence representation of the orthosteric binding pockets, which is essential for evaluating the fit of the designed ligands.
Blind docking was performed via the CB-Dock2 server, utilizing the CurPocket algorithm for automated cavity detection. The primary docking simulations were conducted using AutoDock Vina.